Quadruplex folding promotes the condensation of linker histones and DNAs via liquid-liquid phase separation

Masahiro Mimura[†,‡], Shunsuke Tomita[*,‡], Yoichi Shinkai[⁑], Takuya Hosokai[⁂], Hiroyuki Kumeta[//], Tomohide Saio[¶], Kentaro Shiraki[†], Ryoji Kurita [*,†,‡,§]

[†]Faculty of Pure and Applied Sciences, University of Tsukuba, 1-1-1 Tennodai, Tsukuba, Ibaraki 305-8573, Japan, [‡]Health and Medical Research Institute, National Institute of Advanced Industrial Science & Technology (AIST), 1-1-1 Higashi, Tsukuba, Ibaraki 305-8566, Japan, [⁑]Biomedical Research Institute, AIST, 1-1-1 Higashi, Tsukuba, Ibaraki 305-8566, Japan, [⁂]National Metrology Institute, AIST, 1-1-1 Higashi, Tsukuba, Ibaraki 305-8565, Japan, [//]Faculty of Advanced Life Science, Hokkaido University, Sapporo, Hokkaido, 060-0810, Japan, [¶]Graduate School of Chemical Sciences and Engineering, Hokkaido University, Sapporo, Hokkaido, 060-8628, Japan, [§]DAILAB, DBT-AIST International Center for Translational and Environmental Research (DAICENTER), AIST, 1-1-1 Higashi, Tsukuba, Ibaraki, 305-8565, Japan, [*]Corresponding author

KEYWORDS, Chromatin condensation, G-quadruplex, Histone, Liquid-liquid phase separation

ABSTRACT: Liquid-liquid phase separation (LLPS) of proteins and DNA has recently emerged as a possible mechanism underlying the dynamic organization of chromatin. We herein report the role of DNA quadruplex folding in liquid droplet formation via LLPS induced by interactions between DNA and linker histone H1 (H1), a key regulator of chromatin organization. Fluidity measurements inside the droplets, binding assays using G-quadruplex-selective probes, and structural analyses based on circular dichroism demonstrated that quadruplex DNA structures, such as the G-quadruplex and i-motif, promote droplet formation with H1 and decrease molecular motility within droplets. The dissolution of the droplets in the presence of additives and the LLPS of the DNA structural units indicated that in addition to electrostatic interactions between the DNA and the intrinsically disordered region of H1, π-π stacking between quadruplex DNAs could potentially drive droplet formation, unlike in the electrostatically driven LLPS of duplex DNA and H1. According to phase diagrams of anionic molecules with various conformations, the high LLPS ability associated with quadruplex folding arises from the formation of interfaces consisting of organized planes of guanine bases and the side surfaces with high charge density. Given that DNA quadruplex structures are well documented in heterochromatin regions, it is imperative to understand the role of DNA quadruplex folding in the context of intranuclear LLPS.

Introduction

Genomic DNA in eukaryotic cells wraps around histone protein cores to form nucleosomes, which are further compacted into chromatin.[1] The level of chromatin condensation is closely related to gene transcription;[2] heterochromatin is a tightly packed form that is inaccessible to polymerases and thus inactivates gene transcription, whereas gene transcription is activated in euchromatin, in which the nucleosomes are loosely packed.[3] Chromatin undergoes highly dynamic changes in its condensed structure during a cell cycle. However, the mechanisms that govern the organization of chromatin remain largely unknown.

Liquid-liquid phase separation (LLPS) has emerged as a possible mechanism for the control of chromatin organization through the promotion of nucleosome packing.[4] Biological LLPS is a process in which solutions of biomacromolecules spontaneously separate into two phases.[5,6] In such events, one phase is usually a small-volume droplet-like phase in which the biomacromolecules are concentrated in aqueous media, while the other is the surrounding phase, which is depleted of the biomacromolecules.[7] Multivalent weak intermolecular interactions involving intrinsically disordered regions (IDRs) of proteins, such as electrostatic, cation-π, and π-π interactions, play crucial roles in LLPS.[5,6] For instance, binding of the IDR-containing heterochromatin protein HP1α to the histone H3K9 methylation site induces LLPS in specific domains of heterochromatin.[8,9] LLPS also occurs in euchromatin regions that are rich in acetylated histone tails when the transcriptional regulator protein BRD4, which contains a long IDR, is co-localized.[10,11]

Thus, the nature of the relationship between LLPS-mediated chromatin-condensation and proteins is gradually determined.

Several reports have indicated that DNA is also involved in the LLPS associated with chromatin condensation. The length of the inter-nucleosome linker DNA strongly affects the LLPS of nucleosome arrays.[10] Double-stranded DNA induces LLPS in the presence of histone H1,[12] which is capable of regulating chromatin organization via binding to inter-nucleosome linker DNA. However, knowledge regarding the structure of the DNA involved in LLPS-mediated chromatin-condensation is still very limited. Therefore, in this work, we have focused on the secondary structures of DNA, especially the most common G-quadruplex structure.[13]

G-quadruplex is a stacking planar structure formed through Hoogsteen hydrogen bonds between four guanine residues (Figure 1A).[13] Guanine-rich sequences with the potential to fold into the G-quadruplex structure are frequently observed in oncogene promoter sequences and telomere regions, which are known as quadruplex clusters or G4 clusters,[14,15] where they may promote or inhibit the access of transcriptional factors or telomere binding proteins.[16,17] Recently, it has been revealed that G-quadruplex sequences are also abundant in heterochromatin region;[18] however, the role of these sequences on chromatin condensation has not been clarified. Thus, we attempted to elucidate the relationship between the G-quadruplex DNA structure and the LLPS of chromatin constituents using a variety of sequences that are capable of forming quadruplex structures. The presented findings will facilitate the understanding of the role of G-quadruplex structures in the cell nucleus and chromatin condensation.

Results and Discussion

LLPS of G-quadruplex-forming ssDNA with H1

To investigate the effect of G-quadruplex formation on LLPS in the context of chromatin condensation, we chose histone H1 (H1) and various single-stranded DNA (ssDNA) sequences. H1 controls the packing density of nucleosomes via non-specific electrostatic interactions between its positively charged lysine-rich IDR at its C-terminal and negatively charged DNA (Figure 1B).[19] Shakya *et al.* recently reported that among histone proteins, H1 has the highest ability to form droplets with DNA via LLPS.[20] Four 22 nt ssDNA sequences were initially prepared (Figure 1C): an oncogene *c-myc* promoter sequence that can fold into a parallel G-quadruplex structure (Pu22)[21]; sequences in which one or two of the successive guanines of Pu22 were replaced with adenine (Pu22-1 and Pu22-2, respectively); and a simple repeat of deoxyadenylic acid (poly(dA)) with a random coil structure. The nucleotides are arranged an all-*anti* configuration in the parallel forms of G-quadruplexes, while the antiparallel forms contain nucleotides in both *syn* and *anti* configurations (Figures 1A and S1A). The secondary structure of each ssDNA was examined by circular dichroism (CD) measurements, which revealed that with decreasing number of guanines, the content of G-quadruplex structures decreased (Pu22 to Pu22-1), whereby Pu22-2 exhibits a random coil-like structure (for details, see section 3 of the Supporting Information).

The turbidity of the aqueous solutions of the guanine-containing sequences (Pu22, Pu22-1, and Pu22-2) increased upon addition of H1 up to a certain concentration ([H1]/[ssDNA] = 0.2-0.4) (Figure 2A), indicating that interactions between the ssDNA sequences and H1 resulted in the formation of large assemblies. Interestingly, the maximum turbidity values of the solutions increased with the number of continuous guanines in the ssDNA sequence (Pu22 > Pu22-1 > Pu22-2). The decreased turbidity at high concentrations of H1 probably results from repulsive forces that arise from the excess of positive charge;[12,23] thus, electrostatic interactions between the cationic H1 and anionic ssDNA are presumably a dominant force in the formation of the assemblies. However, although poly(dA), like the other ssDNA sequences, is anionic, the poly(dA) solution did not exhibit an apparent increase in turbidity upon addition of H1.

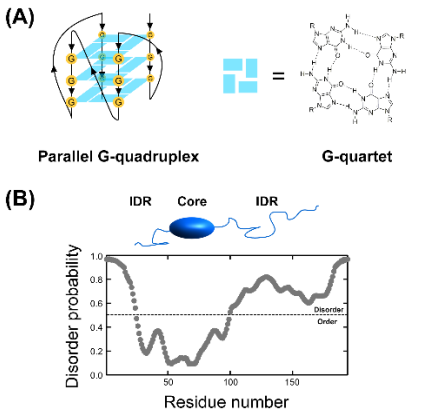

Name	Sequence (5'→3')	Structure
Pu22	TGAGGGTGGGTAGGGTGGGTAA	Parallel G-quadruplex
Pu22-1	TGAGGATGGATAGGATGGATAA	Parallel G-quadruplex (partial)
Pu22-2	TGAGAATGAATAGAATGAATAA	Random
poly(dA)	AAAAAAAAAAAAAAAAAAAAA	Random
22AG	AGGGTTAGGGTTAGGGTTAGGG	Anti-parallel G-quadruplex
22CT	CCCTAACCCTAACCCTAACCCT	i-motif
$22CT_{shuffle}$	CTCACACTCACACTCACACTCC	Random
$dsDNA_{11}$	TGAGGGTGGGT*	Double helix

* One of the sequences constituting the duplex is shown

Figure 1. Sequence and higher order structure of the molecules used in this study. (A) Schematic illustration of the parallel G-quadruplex DNA structure (left), which consists of stacked G-quartets (right). (B) Disorder probability of the H1 structure as predicted using the Protein DisOrder prediction System (PrDOS).[22] Regions of the sequence that exhibit a score bigger than 0.5 are defined as intrinsically disordered regions (highlighted in light blue). The sequence of H1 from bovine thymus was obtained from Uniprot code Q0IIJ2. (C) Sequences and structures of the ssDNA used in this study.

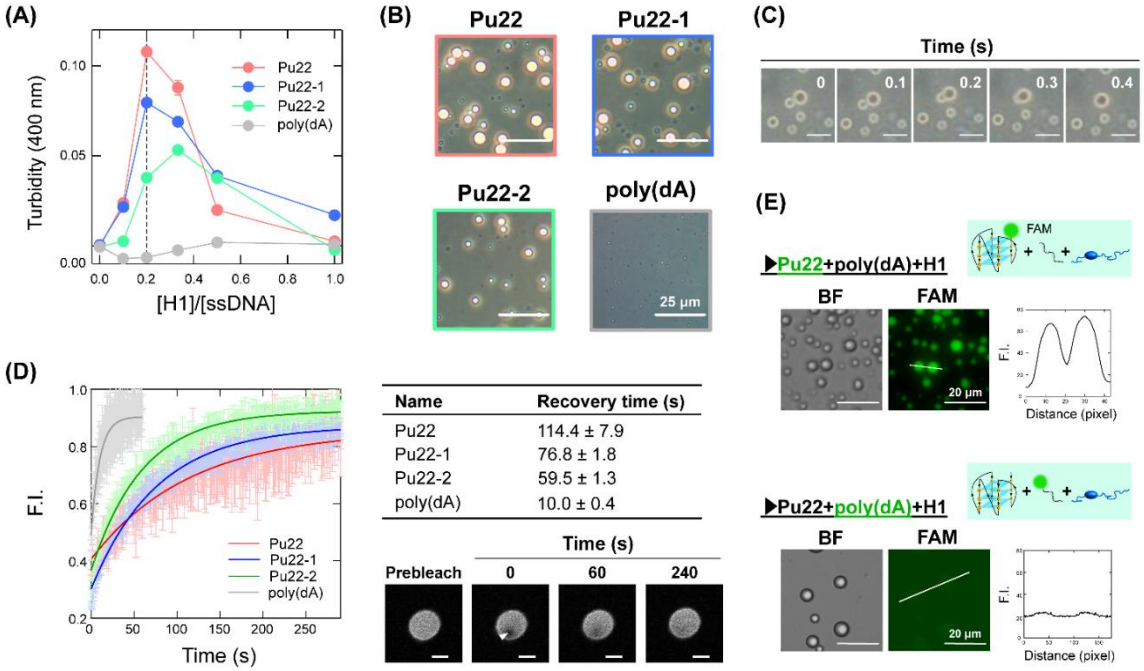

Figure 2. Liquid-like droplets of G-quadruplex-forming ssDNA with H1. (A) Turbidity of solutions that contain various ssDNA sequences (10 μM) and H1 (0-10 μM). (B) Phase-contrast-microscopy images of solutions that contain ssDNA (10 μM) and H1 (2 μM); scale bar = 25 μm. (C) Fusion process of the Pu22/H1 droplets; scale bar = 10 μm. (D) Left: FRAP recovery curves for the different ssDNA structures. Right: recovery times of fluorescence calculated by exponential fitting (colored lines; N = 3), and fluorescence images obtained during the FRAP measurement of a Pu22/H1 liquid droplet. The white arrowhead indicates the bleaching site; scale bar = 5 μm. (E) Selectivity of the ssDNA sequences for the droplet formation with H1. Either Pu22 or poly(dA) was modified with FAM, and both (10 μM) were mixed with H1 (2 μM). The fluorescence intensity along the white line was quantified from the brightness of each pixel; scale bar = 20 μm. All experiments were carried out in 10 mM Tris-EDTA buffer (pH = 7.4).

Spherical assemblies were observed via phase-contrast microscopy for all turbid ssDNA solutions ([H1]/[ssDNA] = 0.2; Figure 2B), similarly to our recent studies of cationic protein/anionic polymer pairs.[24,25] Time-lapse images showed rapid, sub-millisecond fusion of the assemblies (Figure 2C). This behavior indicates that these assemblies are not gel-like aggregates, but instead liquid-like droplets with highly fluid properties, as have been observed for other phase-separating proteins.[26] Consistent with the turbidity measurements (Figure 2A), the size of the observed droplets decreased with decreasing number of continuous guanines in the ssDNA sequence. In the case of poly(dA), only small droplets (diameter < 1.0μm) were formed. Similar behavior was observed for other ssDNA sequences, including an anti-parallel G-quadruplex sequence present in telomeric regions (22AG), its derivatives, and a simple repeat of deoxythymidylic acid (poly(dT)) (Figure S1). Thus, ssDNA sequences capable of forming G-quadruplex are likely to have a high ability to form droplets with H1.

The effect of the ssDNA sequence on the fluidity inside the droplet was compared using fluorescence recovery after photobleaching (FRAP), which is a common method for evaluating the motility of molecules inside the droplets.[27] The diffusion rate of the carboxyfluorescein (FAM)-modified ssDNA sequences increased with decreasing number of continuous guanines [poly(dA) > Pu22-2 > Pu22-1 > Pu22], i.e., in the opposite order of the content of quadruplex structures (Figure 2D). Interestingly, the density of the ssDNAs inside the droplet was correlated with their motility (Figure S2), i.e., the higher the G-quadruplex content, the lower the density inside the droplet, despite the stronger intermolecular interactions inside the droplet. Therefore, the G-quadruplex folding also controls the motility and density of the molecules inside the resulting droplets, which could potentially affect cellular functions such as the inhibition of gene transcription.

To study the sequence selectivity of the droplet formation, either Pu22 or poly(dA) was labeled with FAM, and then both were mixed with H1. When Pu22 was labeled, the inside of the droplet emitted strong fluorescence, whereas the fluorescence inside and outside of the droplet was comparable for labeled poly(dA) (Figure 2E), suggesting sequence selectivity not only in the formation of droplets with H1, but also in the incorporation of ssDNA into the resulting droplets.

Based on these results, it seems feasible to conclude that ssDNA sequences that can fold into G-quadruplex structures plays a significant role in (i) the generation of LLPS through

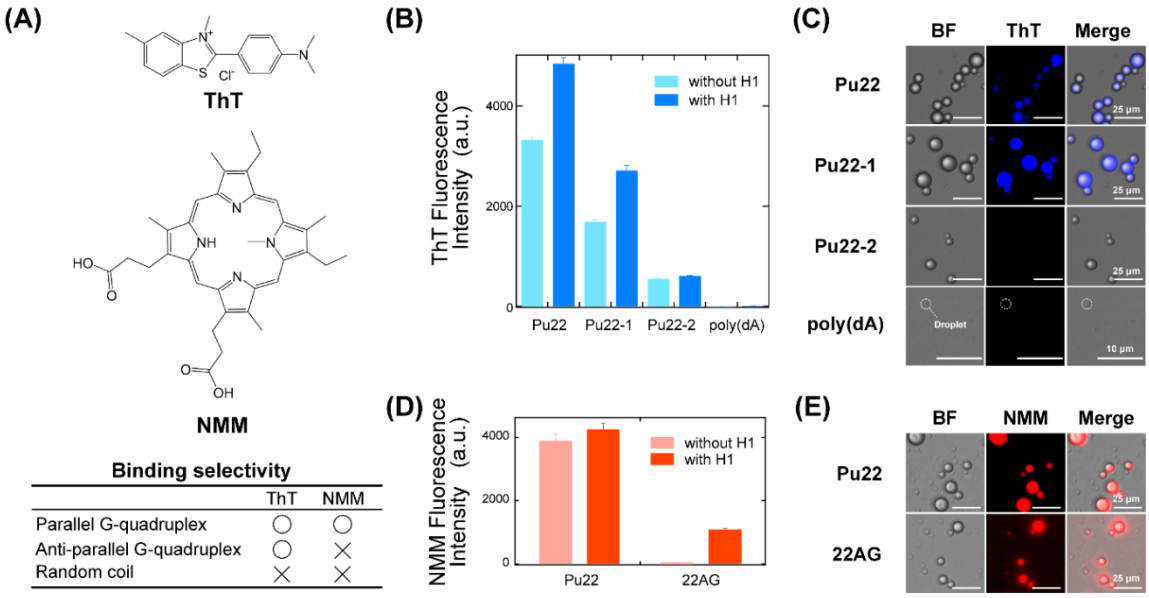

Figure 3. Analysis of G-quadruplex structures inside the liquid droplets using fluorescent molecular probes. (A) Chemical structures of the fluorescent probes ThT and NMM, which exhibit greatly enhanced fluorescence upon their selective binding to G-quadruplex structures. The binding selectivity of ThT and NMM is taken from refs [28] and [29], respectively. Fluorescence intensity of (B) ThT and (D) NMM in solutions that contain ssDNA (10 μM) with or without H1 (2 μM). Fluorescence microscopy images of ssDNA/H1 liquid droplets after the addition of (C) ThT and (E) NMM; scale bar = 25 μm (10 μm for poly(dA)).

interactions with H1, (ii) the motility and density of the molecules inside the formed droplets, and (iii) the ability of the droplets to incorporate other ssDNAs.

G-quadruplex folding within liquid-like droplets

The stability of the G-quadruplex structure is affected by protein binding.[17] Since the components of the droplets formed through LLPS are generally concentrated within the droplets by a factor of several to several hundred compared to the surrounding phase,[10,30] the G-quadruplex content might fluctuate due to the presumably high concentration of H1 inside the droplets. Therefore, we investigated the folding state of the ssDNA within the droplet using two fluorogenic probes that selectively bind to G-quadruplex structures, thioflavin T (ThT) and *N*-methylmesoporphyrin IX (NMM) (Figure 3A). ThT binds to G-quadruplex structures regardless of their configration,[28] while NMM recognizes only parallel-folded G-quadruplexes.[29] These probes are almost nonfluorescent in aqueous solution, but exhibit strong emission when bound to G-quadruplex structures.

In the absence of H1, the overall fluorescence intensity of the solutions in the presence of ThT follows the order Pu22 > Pu22-1 > Pu22-2 >> Poly(dA), i.e., the abundance of G-quadruplex structures increases with increasing number of successive guanines in the ssDNA sequence (Figure 3B; for the fluorescence spectra, see Figure S3A). The fluorescence intensity of ThT after the droplet formation is comparable for the Pu22-2/H1 or poly(dA)/H1 solutions, while that of the Pu22/H1 and Pu22-1/H1 solutions increases 1.5- and 1.6-fold, respectively (Figure 3B). These fluorescence enhancements were not due to changes in the dielectric constant within the droplets, peak shifts, or changes in the fluorescence lifetimes, but instead to the enhanced formation of the G-quadruplex structure to which ThT can bind (for details, see section 4 of the Supporting Information).

Fluorescence microscopy images of the Pu22 and Pu22-1 solutions showed significant fluorescence inside the droplets (Figure 3C), demonstrating that the binding of ThT to the G-quadruplex occurred mainly inside the droplets. In contrast, the Pu22-2 and poly(dA) solutions exhibited very weak fluorescence. We found that other fluorescent dyes (8-anilino-1-naphthalenesulfonic acid, Nile red, and rhodamine 6G) tended to be concentrated in the ssDNA/H1 droplets, regardless of the dye structure or ssDNA sequence (Figure S4). Unlike these dyes, in addition to being concentrated in the ssDNA-rich droplets, ThT must be bound to the G-quadruplex in order to emit visible fluorescence, as indicated in section 4 of the Supporting Information.

The CD spectra of the droplet suspensions and condensed phases supported the possibility of the promotion and maintenance of G-quadruplex folding inside the droplets (for details, see section 5 of the Supporting Information). The measurements of the condensed phase using high-resolution magic angle spinning nuclear magnetic resonance (HR-MAS-NMR), which is a suitable technique for the NMR measurement of samples with high viscosity,[31] suggested that the conformation of quadruplex Pu22 inside the droplets may be polymorphic within the range to which

G-quadruplex specific probes can bind (for details, see section 5 of the Supporting Information).

The origin of the enhancement of the G-quadruplex folding was explored using two model cationic polymers instead of H1: a simple repeat poly-L-lysine (PLL), and PLL with a polyethylene glycol chain, which inhibits droplet growth (for details, see section 6 of the Supporting Information). Briefly, the results suggest that one of the dominant factors was the direct non-specific interactions between polycationic chains and ssDNAs. Such interactions could potentially lead to suppression of the inter- and intramolecular repulsion of ssDNAs by neutralization of the phosphate groups and subsequent promotion of nucleobase stacking. Another possibility is that the molecular crowding causes dehydration of G-quadruplex structures, which stabilizes this conformation.[32] The dense, crowded environment inside the droplets may also lead to enhanced folding.

In the case of a telomere-derived sequence (22AG) that is capable of folding into an anti-parallel G-quadruplex structure, ThT gave results similar to Pu22 (Figure S3B), whereas NMM exhibited interesting behavior. Aqueous solutions of Pu22 showed similar strong fluorescence with or without H1 after the addition of NMM, which is specific to parallel-type G-quadruplexes (Figure 3D), indicating that the parallel G-quadruplex structure of Pu22 is not significantly denatured by H1. On the other hand, substantial NMM emission was observed from the entire solution of anti-parallel 22AG only after droplets were formed by the addition of H1. Similar to the emission of ThT, that of NMM was concentrated inside the droplets for both ssDNA sequences (Figure 3E). The enhancement in the fluorescence after droplet formation for 22AG suggests that the G-quadruplex structures of 22AG transitioned from the anti-parallel to the parallel form. The CD spectra of the condensed phases also indicate the possibility of the structural transition (Figure S18B). Similar to the enhanced folding of Pu22, this structural transition seems to be mainly due to the interaction with the cationic tail of H1 (for details, see section 6 of the Supporting Information), but the molecularly crowded environments might also be significant.[33] It has been reported that the anti-parallel to parallel transition in telomere-derived ssDNA inhibits telomerase processability.[33] Thus, if transition of the G-quadruplex structures of 22AG is coupled to the droplet-formation-inducing interaction with H1, it was presumably involved in the telomere activity switching mechanism in the cell nucleus.

Generality of the promotion of LLPS by the quadruplex conformation

To clarify the generality of the promotion of LLPS by quadruplex structures in ssDNA, we tested another quadruplex structure formed by successive cytosine bases, the so-called i-motif (Figure 4A).[34] As in the case of G-quadruplex, the increase in turbidity upon addition of H1 was greater for an i-motif-forming sequence (22CT) than for a shuffled variant of this sequence in which the cytosines are not successive ($22CT_{shuffle}$) (Figure 4B). Consistent with the turbidity results, the droplets formed by 22CT were significantly larger than those formed by $22CT_{shuffle}$ (Figure 4B). The CD spectrum of the condensed phase suggested that the folding of 22CT into the i-motif was promoted by the process of droplet formation (Figure S18C).

Thus, the dependence of the phase separation behavior on the arrangement of the ssDNA suggests that the quadruplex structure is important in promoting LLPS with H1, regardless of the kind of constituent nucleobases. In addition, we found that the droplet formation between quadruplex-forming ssDNAs and polycationic chains such as H1 was synchronized with structural stabilization or transition.

Driving forces for the formation of droplets between DNAs and H1

Subsequently, we investigated the reason that the quadruplex structures promote droplet formation between H1 and ssDNA. To gain further insight into the driving forces of droplet formation, we examined the effects of additives (NaCl and 1,6-hexanediol) that can inhibit electrostatic and hydrophobic interactions, respectively,[35] by adding them to solutions containing the DNA/H1 liquid droplets. For comparison, we also used 11-base pairs of double-stranded DNA ($dsDNA_{11}$; Figure 1C), which had the same total number of nucleobases as the other ssDNAs. The duplex structure has some features similar to those of the quadruplex structure: (i) nucleobases embedded by base pairing, (ii) a relatively rigid structure, and (iii) LLPS when mixed with H1.[12,36]

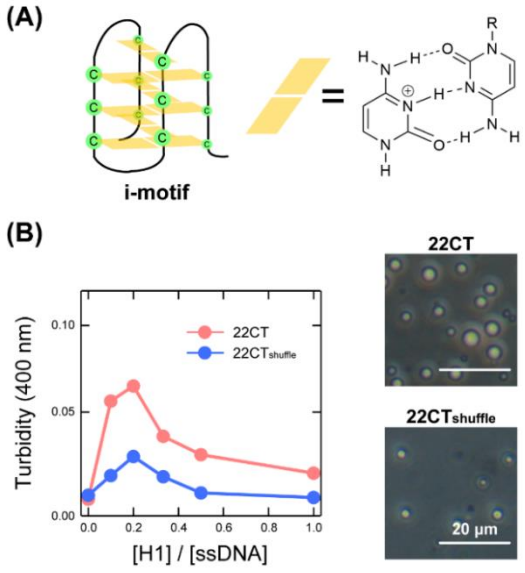

Figure 4. Droplet formation in a solution that contains cytosine-based quadruplex structures and H1. (A) Schematic illustration of the i-motif structure and the DNA sequences used in this experiment. (B) Formation of liquid droplets in solutions of i-motif DNA (22CT) or a shuffled sequence (22CTshuffle) with H1 (2 μM); scale bar = 20 μm.

NaCl markedly reduced both the turbidity of the solution and the droplet size (Figures 5A and S5). In all DNAs, the droplets disappeared completely at higher-than-physiological NaCl concentrations (~300 mM), as observed previously.[12] This result demonstrates that the electrostatic interactions between the cationic C-terminus of H1 and the anionic phosphate groups of DNAs are the dominant driving force in the generation of LLPS.

Unexpectedly, the droplets consisting of the various G-quadruplex-forming ssDNAs gradually dissolved as the 1,6-hexanediol concentration was increased, whereas the turbidity of the solutions containing droplets formed by $dsDNA_{11}$ did not change at all, even in the presence of 20% 1,6-hexanediol (Figures 5B and S6). This result suggests that hydrophobic interactions contribute substantially to the stabilization of the droplets of G-quadruplex-forming ssDNAs, but not those of $dsDNA_{11}$. To better understand the nature of these hydrophobic interactions, the relationship between LLPS and the nucleotide-monophosphate (NMP) DNA structural units was examined. Among the four NMPs, only guanine monophosphate (GMP) caused droplet formation in the presence of both H1 and high concentrations of PEG, which is known to promote the generation of LLPS (Figures 5C and S7).[37]

Guanine has the lowest energy of stacking interaction with both aromatic amino acids[38] and nucleobases[39] among the nucleobases. Considering the fact that H1 contains only several aromatic amino acids (only two Phe and three Tyr in 194 aa), more stable stacking of the guanine bases may explain the results observed for the various NMPs, i.e., it is plausible that the hydrophobic π-π stacking of guanine bases is a significant factor for the LLPS of G-quadruplexes.

Taken together, (i) electrostatic interactions between the DNAs and the intrinsically disordered region of H1 and (ii) π-π stacking between quadruplex DNAs drove droplet formation between G-quadruplex DNA and H1, unlike in the electrostatically driven LLPS of duplex DNA and H1. In addition to electrostatic interactions, π-π interactions are known to be significant in protein phase separation to direct the state of the assembly towards liquid-like droplets rather than gel-like aggregates.[44] Hydrogen-bonding interactions between partially exposed guanine bases and lysine residues[45] of H1, and cation-π interactions, which stabilize a wide variety of intracellular droplets,[46,47] between the same pairs may also contribute to the stability of the DNA/H1 droplets. These considerations were also supported by an experiment using ssDNA with shuffled variants of G-quadruplex-forming sequences (for details, see Section 7 of the Supporting Information).

Role of structural rigidity on the formation of droplets between DNAs and H1

Although the key driving forces have been identified, the effects of the structuring of ssDNA on the formation of droplets are still puzzling. It is generally believed that biological

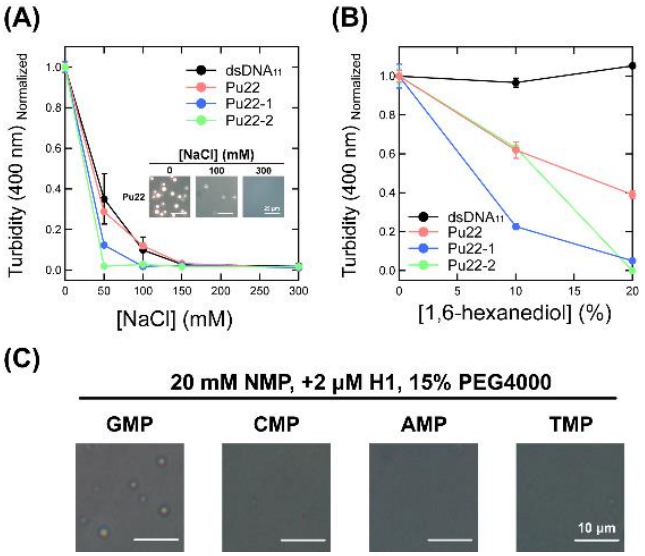

Figure 5. Physicochemical properties of the DNA/H1 liquid droplets. (A and B) Turbidity of solutions of the ssDNA/H1 liquid droplets in the presence of (A) 0–300 mM NaCl or (B) 0-20% 1,6–hexanediol. Insets are phase-contrast images of the Pu22/H1 liquid droplets in the presence of NaCl; scale bar = 25 μm. (C) Phase-contrast microscopy images of solutions that contain 20 mM NMP, 2 μM H1, and 15% PEG4000; scale bar = 10 μm.

LLPS requires flexible sequences (e.g., IDR).[48] It has been reported that when DNAs are stiffened by the formation of secondary structures such as double strands or loops, they form gel-like aggregates rather than liquid-like droplets in the presence of cationic macromolecules,[49,50] or are excluded from protein droplets.[51] The high droplet formation ability of the compact and rigid quadruplex folding structure seems to be inconsistent with these findings.

Therefore, the effect of structuring was investigated by comparing the LLPS of flexible poly(dA) and a highly rigid, hydrophilic, spherical poly(amidoamine) (PAMAM) dendrimer with 64 carboxyl groups on its surface. According to the phase diagrams of H1 vs. NaCl concentration (Figures 6, S8 and S9), Pu22, whose rigidity is intermediate between those of dsDNA[40] and the PAMAM dendrimer,[52] clearly exhibited the highest phase separation ability (Figure 6). This result implies that structural flexibility is not necessarily an essential factor for LLPS with H1. The PAMAM dendrimer can also be considered to be a model of polyanionic proteins, such as the histone chaperone prothymosin alpha, which can bind and condense H1 without LLPS,[53] and our result may be similar to the behavior of such proteins.

The observed high LLPS ability of quadruplex folding structures is possibly due to the formation of interfaces consisting of organized top/bottom planes of guanine bases and the side surfaces with high charge density. As recently reported, interactions between interfaces formed by structuring can promote LLPS.[54] Short dsDNAs also undergo

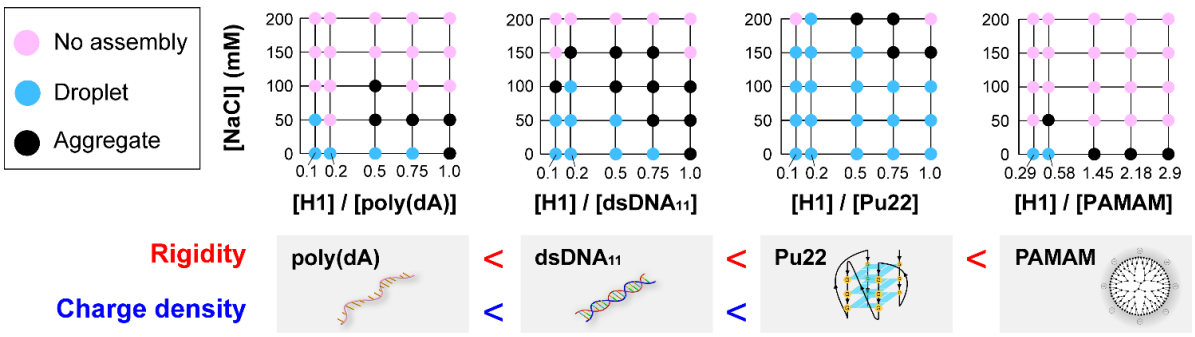

Figure 6. Phase diagrams of aqueous mixtures of H1 and various anionic molecules. The solution states are plotted as the NaCl concentration vs. the molar mixing ratio of H1 to DNAs (10 μM) or PAMAM (3.44 μM). The concentration range of PAMAM (64 anions per molecule) was chosen to have the same charge as the DNA solution (22 anions per molecule). Pink dots: no phase separation; blue dots: liquid-liquid phase separation; black dots: solid-liquid phase separation (i.e., aggregation). The order of the rigidity and charge density of the molecules was based on references 40 and 41, and 42 and 43, respectively.

hierarchical self-assembly by end-to-end stacking of base pairs at the terminal interfaces upon droplet formation with polycations.[55] The G-quadruplex exhibits more open and wider stacking interfaces compared to the duplex, and DNAs with quadruplex structures tend to stack intermolecularly in the longitudinal direction at high concentrations.[56,57] These characteristics explain the smaller contribution of hydrophobic interactions in the duplexes compared to that in the G-quadruplexes. Indeed, the phase diagrams showed that Pu22 droplets appeared to be more tolerant to salts than $dsDNA_{11}$ droplets (Figures 6 and S10). This difference should be attributed to improved stability due to hydrophobic inter-nucleobase stackings provided by the upper and lower surfaces of G-quartets. Turbidity measurements (Figure 2A) showed that one H1 molecule bound to multiple ssDNAs. This bridging of ssDNAs by H1 likely contributed to the facilitation of the stacking, and eventually stabilized the intermolecular G-quadruplex formation.

The correlation between the LLPS ability of DNAs with the same number of charges [Pu22, $dsDNA_{11}$, and poly(dA)] and charge density (Figure 6) also suggests the importance of increasing the charge density via structuring. In addition to the planar interfaces preferred for π-π stacking on the top and bottom surfaces, the formation of high-charge-density interfaces on the side surfaces that allow strong electrostatic contacts[58] provides unique features favorable for droplet formation. We thus concluded that the densification of the electrostatic and stacking interactions via the formation of such structures is a key to the high LLPS ability of quadruplex folding structures.

The possible existence of G-quadruplex droplets in the cell nucleus is suggested by the fact that the droplets formed by G-quadruplexes became larger with increasing molecular concentration, even at physiological ionic strength, unlike random structured DNA (Figure S11). The quadruplexes in the nucleus are inhomogeneously distributed depending on the surrounding environment and protein binding. For example, G-quadruplex DNAs and RNAs are concentrated in the promoter and telomere regions of specific genes to form G-quadruplex clusters.[14,15] The concentrations of G-quadruplex DNAs and RNAs thus formed in the nucleus could potentially exceed the thresholds of LLPS locally and transiently, and could be involved, for example, in H1-mediated chromatin LLPS that changes over time.[36] Careful observations of quadruplex DNAs in cells from the perspective of LLPS will shed new light on the role of quadruplex DNAs.

Conclusion

In summary, we have demonstrated that the formation of quadruplex structures in single-strand DNA (ssDNA), including guanine-based parallel and anti-parallel G-quadruplexes and cytosine-based i-motif structures, promotes the formation of liquid-like droplets with linker histone H1 via liquid-liquid phase separation (LLPS). The quadruplex folding is maintained or, in some cases, promoted inside the droplet. Increasing the quadruplex content decreases both the motility and the density of the molecules that comprise the droplet. These droplets are likely formed via not only electrostatic interactions between the anionic ssDNA and the cationic C-terminus of H1, but also via π-π interactions between the quadruplex structures. Thus, DNA quadruplex structures may be capable of regulating LLPS-mediated dynamic chromatin condensation in the nucleus. DNA and RNA with G-quadruplex structures can selectively interact with nuclear proteins such as fused in sarcoma (FUS) and hnRNPA1, which cause amyotrophic lateral sclerosis (ALS) and tend to phase-separate.[59,60] Accordingly, we expect that the quadruplex structure can act as a hub that regulates biological processes such as chromatin condensation in the nucleus via LLPS.

AUTHOR INFORMATION

Corresponding Authors

Shunsuke Tomita - ORCID: orcid.org/0000-0002-0586-6976;
E-mail: s.tomita@aist.go.jp
Ryoji Kurita - ORCID; orcid.org/0000-0001-5666-9561;
Email: r.kurita@aist.go.jp

Notes

The authors declare no competing financial interest.

ACKNOWLEDGMENT

We thank Prof. Daisuke Miyoshi (Konan University) for fruitful discussions. This study was partially supported by a DAICENTER project grant from the DBT (Govt. of India), a special strategic grant from AIST (Japan), and JSPS KAKENHI grants 18H02383 and 19K22377.

REFERENCES

(1) Kouzarides, T. Chromatin Modifications and Their Function. *Cell* **2007**, *128* (4), 693–705.
(2) Criscione, S. W.; Teo, Y. V.; Neretti, N. The Chromatin Landscape of Cellular Senescence. *Trends Genet.* **2016**, *32* (11), 751–761.
(3) Grunstein, M. Histone Acetylation in Chromatin Structure and Transcription. *Nature* **1997**, *389* (6649), 349–352.
(4) Erdel, F.; Rippe, K. Formation of Chromatin Subcompartments by Phase Separation. *Biophys. J.* **2018**, *114* (10), 2262–2270.
(5) Banani, S. F.; Lee, H. O.; Hyman, A. A.; Rosen, M. K. Biomolecular Condensates: Organizers of Cellular Biochemistry. *Nat. Rev. Mol. Cell Biol.* **2017**, *18* (5), 285–298.
(6) Boeynaems, S.; Alberti, S.; Fawzi, N. L.; Mittag, T.; Polymenidou, M.; Rousseau, F.; Schymkowitz, J.; Shorter, J.; Wolozin, B.; Van Den Bosch, L.; Tompa, P.; Fuxreiter, M. Protein Phase Separation: A New Phase in Cell Biology. *Trends Cell Biol.* **2018**, *28* (6), 420–435.
(7) Iwashita, K.; Mimura, M.; Shiraki, K. Control of Aggregation, Coaggregation, and Liquid Droplet of Proteins Using Small Additives. *Curr. Pharm. Biotechnol.* **2018**, *19* (12), 946–955.
(8) Larson, A. G.; Elnatan, D.; Keenen, M. M.; Trnka, M. J.; Johnston, J. B.; Burlingame, A. L.; Agard, D. A.; Redding, S.; Narlikar, G. J. Liquid Droplet Formation by HP1α Suggests a Role for Phase Separation in Heterochromatin. *Nature* **2017**, *547* (7662), 236–240.
(9) Strom, A. R.; Emelyanov, A. V.; Mir, M.; Fyodorov, D. V.; Darzacq, X.; Karpen, G. H. Phase Separation Drives Heterochromatin Domain Formation. *Nature* **2017**, *547* (7662), 241–245.
(10) Gibson, B. A.; Doolittle, L. K.; Schneider, M. W. G.; Jensen, L. E.; Gamarra, N.; Henry, L.; Gerlich, D. W.; Redding, S.; Rosen, M. K. Organization of Chromatin by Intrinsic and Regulated Phase Separation. *Cell* **2019**, *179* (2), 470-484.e21.
(11) Shin, Y.; Chang, Y.-C.; Lee, D. S. W.; Berry, J.; Sanders, D. W.; Ronceray, P.; Wingreen, N. S.; Haataja, M.; Brangwynne, C. P. Liquid Nuclear Condensates Mechanically Sense and Restructure the Genome. *Cell* **2018**, *175* (6), 1481-1491.e13.
(12) Turner, A. L.; Watson, M.; Wilkins, O. G.; Cato, L.; Travers, A.; Thomas, J. O.; Stott, K. Highly Disordered Histone H1– DNA Model Complexes and Their Condensates. *Proc. Natl. Acad. Sci. U. S. A.* **2018**, *115* (47), 11964-11969.
(13) Burge, S.; Parkinson, G. N.; Hazel, P.; Todd, A. K.; Neidle, S. Quadruplex DNA: Sequence, Topology and Structure. *Nucleic Acids Res.* **2006**, *34* (19), 5402–5415.
(14) Yoshida, W.; Saikyo, H.; Nakabayashi, K.; Yoshioka, H.; Bay, D. H.; Iida, K.; Kawai, T.; Hata, K.; Ikebukuro, K.; Nagasawa, K.; Karube, I. Identification of G-Quadruplex Clusters by High-Throughput Sequencing of Whole-Genome Amplified Products with a G-Quadruplex Ligand. *Sci. Rep.* **2018**, *8* (1), 3116.
(15) Xu, Y.; Suzuki, Y.; Ito, K.; Komiyama, M. Telomeric Repeat-Containing RNA Structure in Living Cells. *Proc. Natl. Acad. Sci. U. S. A.* **2010**, *107* (33), 14579–14584.
(16) Murat, P.; Balasubramanian, S. Existence and Consequences of G-Quadruplex Structures in DNA. *Curr. Opin. Genet. Dev.* **2014**, *25* (1), 22–29.
(17) Paeschke, K.; Simonsson, T.; Postberg, J.; Rhodes, D.; Lipps, H. J. Telomere End-Binding Proteins Control the Formation of G-Quadruplex DNA Structures in Vivo. *Nat. Struct. Mol. Biol.* **2005**, *12* (10), 847–854.
(18) Hoffmann, R. F.; Moshkin, Y. M.; Mouton, S.; Grzeschik, N. A.; Kalicharan, R. D.; Kuipers, J.; Wolters, A. H. G.; Nishida, K.; Romashchenko, A. V.; Postberg, J.; Lipps, H.; Berezikov, E.; Sibon, O. C. M.; Giepmans, B. N. G.; Lansdorp, P. M. Guanine Quadruplex Structures Localize to Heterochromatin. *Nucleic Acids Res.* **2016**, *44* (1), 152-163.
(19) Perišić, O.; Schlick, T. Dependence of the Linker Histone and Chromatin Condensation on the Nucleosome Environment. *J. Phys. Chem. B* **2017**, *121* (33), 7823–7832.
(20) Shakya, A.; King, J. T. Non-Fickian Molecular Transport in Protein–DNA Droplets. *ACS Macro Lett.* **2018**, *7* (10), 1220–1225.
(21) Ambrus, A.; Chen, D.; Dai, J.; Jones, R. A.; Yang, D. Solution Structure of the Biologically Relevant G-Quadruplex Element in the Human c-MYC Promoter. Implications for G-Quadruplex Stabilization. *Biochemistry* **2005**, *44* (6), 2048–2058.
(22) Ishida, T.; Kinoshita, K. PrDOS: Prediction of Disordered Protein Regions from Amino Acid Sequence. *Nucleic Acids Res.* **2007**, *35*, W460-464.
(23) Kurinomaru, T.; Maruyama, T.; Izaki, S.; Handa, K.; Kimoto, T.; Shiraki, K. Protein–Poly(Amino Acid) Complex Precipitation for High-Concentration Protein Formulation. *J. Pharm. Sci.* **2014**, *103* (8), 2248–2254.
(24) Matsuda, A.; Mimura, M.; Maruyama, T.; Kurinomaru, T.; Shiuhei, M.; Shiraki, K. Liquid Droplet of Protein-Polyelectrolyte Complex for High-Concentration Formulations. *J. Pharm. Sci.* **2018**, *107* (10), 2713–2719.
(25) Mimura, M.; Tsumura, K.; Matsuda, A.; Akatsuka, N.; Shiraki, K. Effect of Additives on Liquid Droplet of Protein–Polyelectrolyte Complex for High-Concentration Formulations. *J. Chem. Phys.* **2019**, *150* (6), 064903.
(26) Brangwynne, C. P.; Eckmann, C. R.; Courson, D. S.; Rybarska, A.; Hoege, C.; Gharakhani, J.; Jülicher, F.; Hyman, A. A. Germline P Granules Are Liquid Droplets That Localize by Controlled Dissolution/Condensation. *Science* **2009**, *324* (5935), 1729–1732.
(27) Taylor, N. O.; Wei, M.-T.; Stone, H. A.; Brangwynne, C. P. Quantifying Dynamics in Phase-Separated Condensates Using Fluorescence Recovery after Photobleaching. *Biophys. J.* **2019**, *117* (7), 1285–1300.
(28) Gabelica, V.; Maeda, R.; Fujimoto, T.; Yaku, H.; Murashima, T.; Sugimoto, N.; Miyoshi, D. Multiple and Cooperative Binding of Fluorescence Light-up Probe Thioflavin T with Human Telomere DNA G-Quadruplex. *Biochemistry* **2013**, *52* (33), 5620–5628.
(29) Nicoludis, J. M.; Barrett, S. P.; Mergny, J.-L.; Yatsunyk, L. A. Interaction of Human Telomeric DNA with N-Methyl Mesoporphyrin IX. *Nucleic Acids Res.* **2012**, *40* (12), 5432–5447.

(30) Lin, Y.; Protter, D. S. W.; Rosen, M. K.; Parker, R. Formation and Maturation of Phase-Separated Liquid Droplets by RNA-Binding Proteins. *Mol. Cell* **2015**, *60* (2), 208–219.
(31) Simpson, A. J.; Kingery, W. L.; Shaw, D. R.; Spraul, M.; Humpfer, E.; Dvortsak, P. The Application of ^{1}H HR-MAS NMR Spectroscopy for the Study of Structures and Associations of Organic Components at the Solid- Aqueous Interface of a Whole Soil. *Environ. Sci. Technol.* **2001**, *35* (16), 3321–3325.
(32) Miyoshi, D.; Karimata, H.; Sugimoto, N. Hydration Regulates Thermodynamics of G-Quadruplex Formation under Molecular Crowding Conditions. *J. Am. Chem. Soc.* **2006**, *128* (24), 7957–7963.
(33) Xue, Y.; Kan, Z.-Y.; Wang, Q.; Yao, Y.; Liu, J.; Hao, Y.-H.; Tan, Z. Human Telomeric DNA Forms Parallel-Stranded Intramolecular G-Quadruplex in K+ Solution under Molecular Crowding Condition. *J. Am. Chem. Soc.* **2007**, *129* (36), 11185–11191.
(34) Phan, A. T.; Mergny, J. Human Telomeric DNA: G‐quadruplex, I‐motif and Watson‐Crick Double Helix. *Nucleic Acids Res.* **2002**, *30* (21), 4618‐4625.
(35) Lin, Y.; Mori, E.; Kato, M.; Xiang, S.; Wu, L.; Kwon, I.; McKnight, S. L. Toxic PR Poly-Dipeptides Encoded by the C9orf72 Repeat Expansion Target LC Domain Polymers. *Cell* **2016**, *167* (3), 789-802.e12.
(36) Shakya, A.; Park, S.; Rana, N.; King, J. T. Liquid-Liquid Phase Separation of Histone Proteins in Cells: Role in Chromatin Organization. *Biophys. J.* **2020**, *118* (3), 753–764.
(37) Park, S.; Barnes, R.; Lin, Y.; Jeon, B.-J.; Najafi, S.; Delaney, K. T.; Fredrickson, G. H.; Shea, J.-E.; Hwang, D. S.; Han, S. Dehydration Entropy Drives Liquid-Liquid Phase Separation by Molecular Crowding. *Commun. Chem.* **2020**, *3* (1), 83.
(38) Rutledge, L. R.; Campbell-Verduyn, L. S.; Wetmore, S. D. Characterization of the Stacking Interactions between DNA or RNA Nucleobases and the Aromatic Amino Acids. *Chem. Phys. Lett.* **2007**, *444* (1), 167–175.
(39) Hobza, P.; Šponer, J. Structure, Energetics, and Dynamics of the Nucleic Acid Base Pairs: Nonempirical Ab Initio Calculations. *Chem. Rev.* **1999**, *99* (11), 3247–3276.
(40) Cohen, H.; Sapir, T.; Borovok, N.; Molotsky, T.; Di Felice, R.; Kotlyar, A. B.; Porath, D. Polarizability of G4-DNA Observed by Electrostatic Force Microscopy Measurements. *Nano Lett.* **2007**, *7* (4), 981–986.
(41) Sim, A. Y. L. Nucleic Acid Polymeric Properties and Electrostatics: Directly Comparing Theory and Simulation with Experiment. *Adv. Colloid Interface Sci.* **2016**, *232*, 49–56.
(42) Zhang, Y.; Zhou, H.; Ou-Yang, Z. -C. Stretching Single-Stranded DNA: Interplay of Electrostatic, Base-Pairing, and Base-Pair Stacking Interactions. *Biophys. J.* **2001**, *81* (2), 1133–1143.
(43) Gatto, B.; Palumbo, M.; Sissi, C. Nucleic Acid Aptamers Based on the G-Quadruplex Structure: Therapeutic and Diagnostic Potential. *Curr. Med. Chem.* **2009**, *16* (10), 1248–1265.
(44) Vernon, R. M.; Chong, P. A.; Tsang, B.; Kim, T. H.; Bah, A.; Farber, P.; Lin, H.; Forman-Kay, J. D. Pi-Pi Contacts Are an Overlooked Protein Feature Relevant to Phase Separation. *Elife* **2018**, *7*, e31486.
(45) Czyżnikowska, Ż.; Lipkowski, P.; Góra, R. W.; Zaleśny, R.; Cheng, A. C. On the Nature of Intermolecular Interactions in Nucleic Acid Base-Amino Acid Side-Chain Complexes. *J. Phys. Chem. B* **2009**, *113* (33), 11511–11520.
(46) Alshareedah, I.; Kaur, T.; Ngo, J.; Seppala, H.; Kounatse, L.-A. D.; Wang, W.; Moosa, M. M.; Banerjee, P. R. Interplay between Short-Range Attraction and Long-Range Repulsion Controls Reentrant Liquid Condensation of Ribonucleoprotein–RNA Complexes. *J. Am. Chem. Soc.* **2019**, *141* (37), 14593–14602.
(47) Lin, Y.-H.; Forman-Kay, J. D.; Chan, H. S. Sequence-Specific Polyampholyte Phase Separation in Membraneless Organelles. *Phys. Rev. Lett.* **2016**, *117* (17), 178101.
(48) Uversky, V. N. Intrinsically Disordered Proteins in Overcrowded Milieu: Membrane-Less Organelles, Phase Separation, and Intrinsic Disorder. *Curr. Opin. Struct. Biol.* **2017**, *44*, 18–30.
(49) Shakya, A.; King, J. T. DNA Local-Flexibility-Dependent Assembly of Phase-Separated Liquid Droplets. *Biophys. J.* **2018**, *115* (10), 1840–1847.
(50) Vieregg, J. R.; Lueckheide, M.; Marciel, A. B.; Leon, L.; Bologna, A. J.; Rivera, J. R.; Tirrell, M. V. Oligonucleotide–Peptide Complexes: Phase Control by Hybridization. *J. Am. Chem. Soc.* **2018**, *140* (5), 1632–1638.
(51) Nott, T. J.; Craggs, T. D.; Baldwin, A. J. Membraneless Organelles Can Melt Nucleic Acid Duplexes and Act as Biomolecular Filters. *Nat. Chem.* **2016**, *8* (6), 569–575.
(52) Chen, Z.; Chen, L.; Ma, H.; Zhou, T.; Li, X. Aptamer Biosensor for Label-Free Impedance Spectroscopy Detection of Potassium Ion Based on DNA G-Quadruplex Conformation. *Biosens. Bioelectron.* **2013**, *48*, 108–112.
(53) George, E. M.; Brown, D. T. Prothymosin Alpha Is a Component of a Linker Histone Chaperone. *FEBS Lett.* **2010**, *584* (13), 2833–2836.
(54) Conicella, A. E.; Dignon, G. L.; Zerze, G. H.; Schmidt, H. B.; D'Ordine, A. M.; Kim, Y. C.; Rohatgi, R.; Ayala, Y. M.; Mittal, J.; Fawzi, N. L. TDP-43 α-Helical Structure Tunes Liquid–Liquid Phase Separation and Function. *Proc. Natl. Acad. Sci. U. S. A.* **2020**, *117* (11), 5883–5894.
(55) Fraccia, T. P.; Jia, T. Z. Liquid Crystal Coacervates Composed of Short Double-Stranded DNA and Cationic Peptides. *ACS Nano* **2020**, *14* (11), 15071–15082.
(56) Guittet, E.; Renciuk, D.; Leroy, J.-L. Junctions between I-Motif Tetramers in Supramolecular Structures. *Nucleic Acids Res.* **2012**, *40* (11), 5162–5170.
(57) Vorlíčková, M.; Kejnovská, I.; Sagi, J.; Renčiuk, D.; Bednářová, K.; Motlová, J.; Kypr, J. Circular Dichroism and Guanine Quadruplexes. *Methods* **2012**, *57* (1), 64–75.
(58) Alberti, P.; Mergny, J.-L. DNA Duplex–Quadruplex Exchange as the Basis for a Nanomolecular Machine. *Proc. Natl. Acad. Sci. U. S. A.* **2003**, *100* (4), 1569–1573.
(59) Zhang, Q.-S.; Manche, L.; Xu, R.-M.; Krainer, A. R. HnRNP A1 Associates with Telomere Ends and Stimulates Telomerase Activity. *RNA* **2006**, *12* (6), 1116–1128.
(60) Takahama, K.; Takada, A.; Tada, S.; Shimizu, M.; Sayama, K.; Kurokawa, R.; Oyoshi, T. Regulation of Telomere Length by G-Quadruplex Telomere DNA- and TERRA-Binding Protein TLS/FUS. *Chem. Biol.* **2013**, *20* (3), 341–350.

766 **For Table of Contents Only**

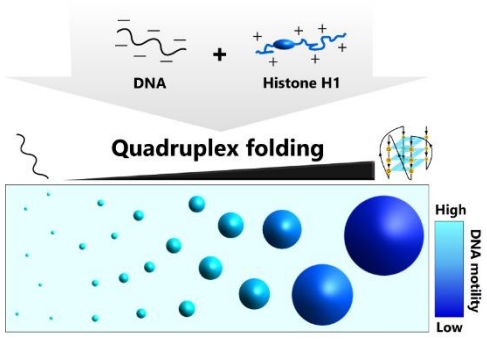

767

768